

## MOLECULARLY IMPRINTED BIOPOLYMER CRYOGELS-LIKE MATERIALS FOR PENICILLIN G RETENTION

Marinela Victoria DUMITRU<sup>1</sup>, Sandu TEODOR<sup>2</sup>, Andreea MIRON<sup>3</sup>, Tanță Verona IORDACHE<sup>4</sup>, Horia IOVU<sup>5\*</sup>, Anita-Laura CHIRIAC<sup>6\*</sup>

*Molecular imprinting is a known method for creating selective binding sites in synthetic or natural polymers using a molecular template. In this context, the study presents the design of novel molecularly imprinted cryogels-like materials based on biopolymers (chitosan and biocellulose), able to act as selective recognition materials for penicillin G retention from aqueous solutions. The prepared molecularly imprinted biopolymer cryogels-like materials were characterized by several techniques to underline their composition and thermal stability. Further on, the swelling trials and the batch rebinding studies helped explaining the stability and behaviour of cryogels like materials in aqueous solutions but also their ability to retain specifically penicillin G.*

**Keywords:** chitosan, biocellulose, molecularly imprinted cryogels-like materials, penicillin G

### 1. Introduction

The use of antibiotics still represents an important tool for treating various diseases. However, antibiotics is also an important class of pollutants frequently found in water and waste waters [1]. In the aid of water pollution, several studies have reported the use of molecularly imprinted polymers (MIPs), which is a class of materials that can be used for removing water pollutants, including antibiotics [2].

Molecular Imprinting (MI) technique is a well-known synthetic approach to obtain materials, capable of imitating biological entities, such as antibodies, biological receptors, antibiotics, etc [3]. For achieving a successful MI, the

<sup>1</sup> PhD student, Faculty of Chemical Engineering and Biotechnologies, University POLITEHNICA of Bucharest, Romania, marinela.dumitru@icechim.ro

<sup>2</sup> Eng., National Institute for Research and Development in Chemistry and Petrochemistry- ICECHIM Bucharest, Romania, teodor.sandu@icechim.ro

<sup>3</sup> PhD student, Faculty of Chemical Engineering and Biotechnologies, University POLITEHNICA of Bucharest, Romania, andreea.miron@icechim.ro

<sup>4</sup> Eng., National Institute for Research and Development in Chemistry and Petrochemistry- ICECHIM Bucharest, Romania, tanta-verona.iordache@icechim.ro

<sup>5</sup> Prof., Advanced Polymer Materials Group, University POLITEHNICA of Bucharest, Romania and Academy of Romanian Scientists, Romania, horia.iovu@upb.ro

<sup>6</sup> Eng., National Institute for Research and Development in Chemistry and Petrochemistry- ICECHIM Bucharest, Romania, anita-laura.radu@icechim.ro

process implies first the formation of a complex between a template molecule (or target molecule) and the functional monomers, using a proper solvent for the dissolution [4]. The subsequent step, for obtaining MIPs, involves the chemical polymerization of the monomer-template complex in the presence of a crosslinking agent. After polymerization, the template is removed, yielding the molecularly imprinted polymer, bearing selective cavities with a high affinity towards the template molecule. This affinity is the result of the shape and arrangement of the functional groups of the monomer unit around the template molecule. Molecularly imprinted polymers are quite often used in the determination of carbohydrates, peptides, amino acids, proteins, as well as in various other fields, where a certain degree of selectivity is required [3-5].

Molecular Selective Synthetic Receptors (MIPs) have many applications in various fields of science, but the most interesting is the biomedical field. In reference [6], several MIPs have been studied, with applications in the medical field, such as selective MIP for the treatment of cholesterol. This study reported that biocompatible membranes were imprinted with uric acid and further used for blood purification. Moreover, it has been observed that both the bioseparation and the biopurification yield have increased considerably. MIPs are both mechanically and chemically stable, having long lifespan, and the cost of their preparation is lower than natural receptors, which makes them suitable for separation processes [8].

Cryogels are matrices of gels, that have different shapes and sizes, prepared from polymerized solutions of polymeric precursors or monomers (hydrophilic and hydrophobic), which are crosslinked and lyophilized [9-11]. Such materials proved to be suitable in separation processes, as a result to their higher strength, mechanical and chemical stability, as well as for tissue engineering or drug delivery. [12-18].

For instance, in paper [9], cryogels were prepared and used for selective adsorption, such as drug release, selective removal of hazardous and toxic compounds from various samples. However, the main disadvantage of cryogels is that they cannot adsorb large amounts due to their small surface area. For this reason, the incorporation of MIP particles into the polymer network of the cryogel helps increase the adsorption capacity, create the selectivity of the adsorption process, and ensure the proper functioning of the separation process. M.V. Konovalova *et al.* [10] also prepared polymeric particles by molecular imprinting technique. These types of materials show selective recognition cavities for an antibiotic model, namely tetracycline (TC). Further on, the selective tetracycline particles were used to prepare a composite cryogel, which was tested in terms of capacity to adsorb TC from aqueous solutions. In this case, the advantages of embedded cryogels with molecularly imprinted particles referred to excellent selectivity for TC and high mechanical strength.

Cellulose is an attractive biopolymer used in the preparation of food grade cryogels and aerogels. It is the most abundant polysaccharide on Earth, is inexpensive and can also be obtained from agro-industrial vegetable by-streams in a closed loop that avoids the generation of large amounts of waste. Biocellulose (BC) is an organic compound and can be obtained from various microorganism such as *Aerobacter*, *Agrobacterium*. BC is used in biomedical applications such as drug delivery, tissue engineering and dental implants [19-21].

Following cellulose, chitin is the second most abundant polymer, and it can be easily transformed into chitosan by its deacetylation. Compared to biological approaches, chemical chitosan production typically results in larger yields and higher deacetylation degree. The chemical process is also cheap, fast, and of low complexity. Yet, chitosan with better mechanical properties can also be produced using biological techniques [22-25].

The benefits of chitosan include its biocompatibility, biodegradability, and antibacterial activity, among others. These qualities make chitosan an extremely appealing biomaterial for use in a variety of biomedical applications, such as tissue engineering, medication administration, vaccine delivery, and the production of medical devices. Furthermore, because chitosan may be produced in a range of formulations, including nanoparticles, nanofibers, scaffolds, hydrogels, membranes, films, and more, it can be used in a number of biomedical applications [27-29].

Thereby, this study was focused on developing molecularly imprinted supermacroporous cryogels-like materials based on natural polymers (chitosan and biocellulose), with retention features towards antibiotics, such as Penicillin G. The molecularly imprinted supermacroporous cryogels-like materials were prepared by physical crosslinking of chitosan with ammonium bicarbonate, which also acted as a foam promoter due to the presence of acetic acid. The rebinding tests proved that molecularly imprinted polymer cryogels-like materials were able to retain high amounts of PG from synthetic aqueous solutions, with satisfying specificity.

## 2. Materials and Methods

### 2.1 Materials

Chitosan and biocellulose were the biopolymers used for the development of the aimed imprinted and non-imprinted cryogels-like materials. In this study, two types of chitosan were used: (i) Commercial Chitosan (CC,  $\geq 75\%$  deacetylation degree,  $M_n = 2.056 \times 10^5$  g/mol, supplied by Sigma Aldrich) and used as received, and (ii) commercial chitin-derived chitosan (CCH) prepared in laboratory (77% deacetylation degree,  $M_n = 4.7291 \times 10^5$  g/mol) according to Miron et al. [30]). The second component of the polymer mixture, namely

biocellulose (BC) was prepared in the laboratory, starting from natural sources (apples), following a fermentation process [31] provided by our collaborator from the University “Politehnica” of Bucharest in the form of a swollen membrane as described by Frone et al. [31]. Penicillin G (PG, purity  $\geq 100\%$ , M = 356 g/mol supplied by Merck), was chosen as the template molecule. Glacial acetic acid (99% supplied by Sigma Aldrich) was used in a mixture with water to prepare a solution (98% H<sub>2</sub>O-2% CH<sub>3</sub>COOH), which was further used for chitosan dissolution. Ammonium bicarbonate (NH<sub>4</sub>HCO<sub>3</sub>, 99.5 % supplied by Sigma Aldrich) has been used mainly as a foaming agent.

## 2.2 Synthesis of molecularly imprinted and non-imprinted cryogel-like materials based on chitosan and biocellulose

MIP and NIP cryogel-like materials were prepared in several steps. In a first stage, the polymer solution was prepared by dissolution of chitosan in acetic acid. Biocellulose was added to the mixture only after full dissolution of chitosan. For samples, MIP 1/NIP 1 and MIP 3/NIP 3, prepared using only chitosan (CC or CCH, respectively), 0.3 g chitosan were dissolved in 12 mL solvent mixture (98% H<sub>2</sub>O and 2% CH<sub>3</sub>COOH), in a weight ratio of 1:40 (Chitosan: solvent mixture). Dissolution was carried out under magnetic stirring (room temperature, 3 hours). For the corresponding samples with chitosan (CC or CCH, respectively) and BC, MIP 2 /NIP 2 and MIP 4 /NIP4, 0.6 g BC was added in a weight ratio chitosan: BC of 1:2. When a homogeneous distribution of polymer(s) in solution was reached, penicillin G was added to the system (wt. ratio chitosan: PG of 1:2), in order to prepare the PG-imprinted cryogels-like materials (MIP1, MIP2, MIP3, MIP4). The corresponding non-imprinted cryogel-like materials (NIP1, NIP2, NIP3, NIP4) were prepared without the addition of PG. Finally, 0.6 g NH<sub>4</sub>HCO<sub>3</sub> of foaming agent was added to the obtained solution, in a weight ratio of 1:2 (chitosan: NH<sub>4</sub>HCO<sub>3</sub>), the mixture being mechanically homogenized with a spatula, until the foaming process was completed. After this stage, the whole composition was kept in the freezer at -20 °C for 120 hours, after which the bulk was cut down to 1 cm<sup>3</sup> samples and subjected to freeze-drying (lyophilization, for 72 h at -55 °C).

All the samples were submitted to a simultaneous purification and template extraction procedure using 25 mL of distilled water/ cycle, in a shaker at a rotational speed of 300 rpm at 25 °C for 1 hour. The degree of purification and the efficiency of the PG extraction procedure was evaluated by analysing the collected residual waters after each washing cycle. The purification and PG extraction was completed after 4 washing cycles, when the supernatants were clear and no signals were recorded in the UV-Vis spectra. The spectra were also compared to that of a reference PG solution of 20 mmol/L, freshly measured, in order to confirm the absence of PG in the supernatants.

### 2.3 Characterisation methods

The FTIR spectra were recorded using a ThermoScientific Summit Pro spectrophotometer, performing 16 scans for each sample, at a resolution of 4 cm<sup>-1</sup>, in the spectral range 4000-400 cm<sup>-1</sup>. The samples were analysed as potassium bromide pellets.

The TGA and DTG curves of the obtained cryogel-like materials were recorded using the TA Q500 instrument. Each sample was heated from 25 to 800 °C, at a heating rate of 10 °C/min, under inert nitrogen gas atmosphere.

### 2.4 Determination of the Swelling Degrees

In order to determine the effect of biopolymers on the water retention capacity of the obtained samples, the swelling degrees (SD) of the cryogel-like materials (NIP1÷NIP4, MIP1÷MIP4) was studied. Each sample was soaked for 3 hours in 10 mL of water, in Falcon tubes, with a capacity of 50 mL, the stirring being ensured by a Multi-Therm Shaker device (Cool-Heat-Shake) Benchmark (200 rpm, 22 °C). The SDs were calculated at different time intervals using equation 1, were  $m_{swelled}$  and  $m_{dried}$  are the mass of the swollen and dried samples (g).

$$SD = \frac{m_{swelled} - m_{dried}}{m_{dried}} \quad (\text{eq. 1})$$

### 2.5 Batch rebinding experiments from synthetic aqueous solution of PG

Binding performances of the prepared cryogel-like materials were evaluated by conducting rebinding experiments to determine the adsorption capacity of MIPs vs. NIPs towards PG. For a proper determination, the desired amount of either NIPs or MIPs, was immersed into vials containing 10 mL solution of 20 mmol/L PG. The supernatants were evaluated in the time interval 0-1440 min by UV-Vis spectroscopy, using an UV-Vis ThermoScientific EVOLUTION 260 Bio Spectrophotometer. The adsorption capacity ( $Q$ ) for MIP and NIP was calculated using eq (2), while the specificity of adsorption was evaluated by calculating the ration between the adsorption capacity of MIP and that of NIP, using eq (3), parameter noted as the Imprinting Factor ( $IF$ ).

$$Q = (c_i - c_f) \cdot V_s / m_p \quad (\text{eq.2})$$

Where:  $Q$  is the adsorption capacity of the cryogel-like materials (mmol/g polymer);  $c_i$  is the initial PG concentration (mmol/L);  $c_f$  is the final solution after adsorption (mmol/L);  $V_s$  is the volume of the solution (L) and  $m_p$  is the mass of the polymer used (g).

$$IF = Q_{MIP} / Q_{NIP} \quad (\text{eq.3}),$$

Where:  $IF$  is the imprinting factor of the cryogel-like materials;  $Q_{MIP}$  is the adsorption capacity of the imprinted cryogel-like materials (mmol/g) and  $Q_{NIP}$  is the adsorption capacity of the non-imprinted cryogel-like materials (mmol/g).

Using the adsorption data, the kinetics of the process was evaluated using a pseudo-second-order model described by Ho and McKay (eq. 4) [32].

$$\frac{1}{q_t} = \frac{t}{q_e} + \frac{1}{k_2 q_e^2} \quad (\text{eq. 4})$$

Where:  $q_e$  and  $q_t$  are the adsorption capacity at equilibrium (mmol/g) and adsorption capacity at time  $t$  (min), and  $k_2$  (g mmol<sup>-1</sup> min<sup>-1</sup>) is pseudo-second-order adsorption rate constant.

### 3. Results and discussion

#### 3.1 FTIR structural analysis

The FTIR spectra of the supermacroporous MIP and NIP cryogel-like materials before and after being washed, are shown in **Fig. 1 (A), (B), (C) and (D)**. For a proper assignment of bands, the FTIR spectra of samples were compared to that of Penicillin G.

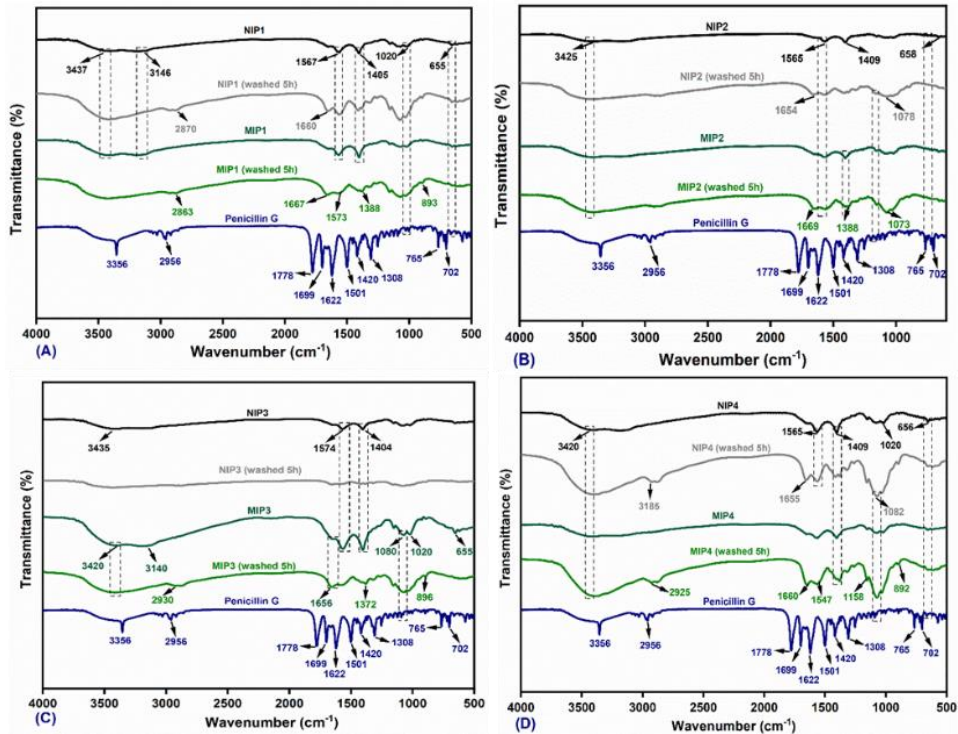


Fig. 1. FTIR spectra for MIP1/NIP1 (A), MIP2/NIP2 (B), MIP3/NIP3 (C), MIP4/NIP4 (D) before and after being washed, compared to that of PG.

The FTIR spectra for samples NIPs and MIPs from Fig. 1 (A, B, C, D) show characteristic bands of both chitosan and biocellulose (i.e., MIP 2/ NIP 2 and MIP 4/ NIP 4 pairs). The band intensity for O-H stretching vibration was observed for NIPs and MIPs at  $3437\text{ cm}^{-1}$  (A),  $3425\text{ cm}^{-1}$  (B),  $3435\text{ cm}^{-1}$  (C),  $3420\text{ cm}^{-1}$  (D), with slight differences from sample to sample. Further on, the stretching vibration for C=O, N-H, O-H, C-O at  $1567\text{ cm}^{-1}$ ,  $1405\text{ cm}^{-1}$ ,  $1020\text{ cm}^{-1}$ , and  $655\text{ cm}^{-1}$ , respectively, characteristic of chitosan structure, are present in all the cryogels-like materials spectra [24]. The biocellulose spectrum is similar to that of chitosan because it contains similar functional groups, except the occurrence of amino group in chitosan [24]. Therefore, for cryogels-like materials with biocellulose content (NIP 2, MIP 2 and NIP 4, MIP 4), the band around  $1158\text{ cm}^{-1}$  for C-O-C and  $1082\text{ cm}^{-1}$  C-O from ether are overlapping with the ones in chitosan [19]. However, the intensities of the bands are different from one sample to another, which may be due to their composition and the fact that two types of chitosan were used. The FTIR spectrum for PG displayed adsorption bands at  $3356\text{ cm}^{-1}$  (O-H Stretching),  $2956\text{ cm}^{-1}$  (C-H Stretching),  $1778\text{ cm}^{-1}$  (C=O group),  $1622\text{ cm}^{-1}$  (C=C isolated),  $1420\text{ cm}^{-1}$  (C-H stretching),  $1308\text{ cm}^{-1}$  (C-H bending) and  $1093\text{ cm}^{-1}$  (O-H bending), respectively [25]. Since the template (PG) shows bands at similar wavenumbers to those corresponding to the cryogel matrix (MIPs), and the amount of PG was rather low, it is rather tricky to confirm the success of the imprinting process by FTIR. However, the spectra of MIPs change before and after washing; some of the bands disappear and some are less intense.

### 3.2. Thermo-gravimetric investigation TGA/DTG

The effect of the template molecule and of the two types of biopolymers on the stability of cryogel-like materials was investigated by thermogravimetric analysis. Interestingly, the MIPs seem to present lower thermal stabilities than the non-imprinted counterparts.

As it may be seen in Fig. 2 (A, B, C, D) the maximum degradation temperatures for samples MIP1÷MIP4 are lower than those registered for the corresponding NIP1÷NIP4, which may be due to decomposition of the template molecule, PG. The maximum degradation temperature of the first stage, registered for all the cryogel-like materials between  $101$  and  $153\text{ }^{\circ}\text{C}$ , may actually be due only to the evaporation of acetic acid, since the measurements were performed for the samples before washing/ extracting the PG. Additionally, it seems that commercial chitosan (used for MIP1/ NIP1 and MIP2/NIP2 pairs) leads to more compact cryogel-like materials, compared to the chitosan prepared in the lab; the evaporation of acetic acid occurs at higher temperatures in these cases. Yet, the DTG curves of all MIPs also reveal the appearance of a small hump after this evaporation step which ends around  $200\text{ }^{\circ}\text{C}$ . Because this hump is not present for

the NIPs, it may be assumed that some decomposition processes of PG occur at this temperature.

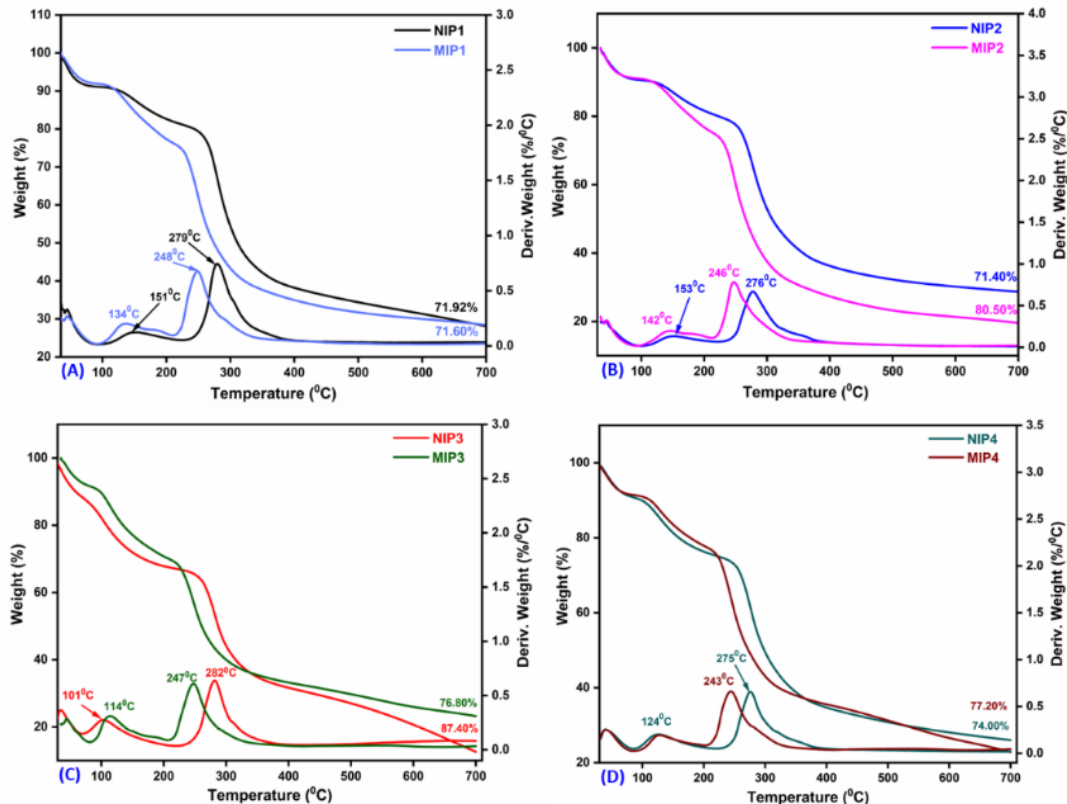


Fig. 2. TGA/DTG curves for NIP1/ MIP1 (A), NIP2/ MIP2 (B), NIP3/ MIP3 (C) and NIP4/ MIP4 (D).

The second step of decomposition also shows an interesting behaviour of cryogel-like materials. It is worth mentioning that NIP cryogel-like materials without biocellulose presented higher mass losses than their MIP counterparts, e.g., 71.92% for NIP1 vs. 71.60% for MIP1 and 87.4% for NIP 3 vs. 76.8% for MIP3, while the cryogels with biocellulose have an opposite behaviour. Thereby, it may be presumed that the chitosan alone has a more pronounced effect on the stability of MIPs.

In conclusion, it can be mentioned that the TGA/DTG results corroborated with the FTIR analysis confirm that the polymeric cryogel-like materials were successfully imprinted with the aimed template molecule, namely PG.

### 3.3. Swelling degrees study

Preliminary studies revealed that cryogel-like materials begin to disintegrate after a few hours in contact with water, due to the fact that the matrix is not chemical crosslinked, and that chitosan is highly soluble in acidic aqueous solutions. For this reason, it was decided to monitor the swelling process in time and determine the optimum contact time. Swelling degrees values, for samples NIP1÷NIP4 and MIP1÷MIP4, are centralized for convenience in *Table 1*.

*Table 1.*  
Swelling degrees (SDs) up to 180 min for the MIP and NIP cryogel-like materials pairs

Time (min)	SD (g H <sub>2</sub> O/g Cryogel)							
	NIP1	MIP1	NIP2	MIP2	NIP3	MIP3	NIP4	MIP4
5	6.91	7.17	7.65	6.82	4.20	4.21	6.92	5.21
15	9.48	9.59	11.92	9.91	5.50	5.44	8.39	6.89
30	17.61	13.39	17.80	14.01	5.89	7.58	12.82	9.95
60	30.78	18.03	15.23	14.27	8.20	12.11	20.10	15.35
120	39.62	21.10	28.14	14.35	8.42	17.61	25.02	19.78
180	39.88	23.36	28.92	-	9.01	20.18	27.29	20.62

As it may be seen from *Table 1*, both imprinted and non-imprinted cryogel-like materials show high swelling capacities. According to this study, it was found that no significant changes may be observed between NIPs and MIPs after 5 minutes. Yet, after 180 min significant differences were revealed, particularly for the SD of MIP3 (20.18) vs. the one registered for NIP3 (9.01), while MIP2 disintegrates only after 180 min. It may also be noted that the cryogel-like materials with biocellulose series 2 and 4, were not as stable as expected. Therefore, it seems that biocellulose does not improve the stability of chitosan-based cryogel-like materials in water. These results are somewhat similar to the ones reported by Dumitru *et al.* [33], in which case the cryogel-like materials with chitosan and biocellulose were reinforced with functionalized clay minerals in order to increase their stability in water.

### 3.4. Batch rebinding experiments and kinetics

The performances of the prepared MIP cryogel-like materials were evaluated by conducting rebinding experiments in the time interval of 0-1440 min. The variance of adsorption capacity in time (Q) and the IF values of cryogels-like materials (NIPs and MIPs) are given Fig. 3 and *Table 2*, respectively. Interestingly, both the MIPs and NIPs have shown an improved stability in water from 180 min to 1440 min, as compared to the SD assessment, which can be associated with the change of the pH for the PG solution, from 5.5 (distilled

water) to 6.5 (20 mmol/L PG solution); thus, preventing chitosan from dissolution [33].

In terms of adsorption capacity (Q), the cryogel-like materials prepared using biocellulose, meaning MIP2 and MIP4, were able to adsorb higher amounts of PG from solution, up to 67 mmol PG/g cryogel-like materials, compared to the ones with chitosan alone (MIP1 and MIP3), i.e., approximately 40 mmol PG/g cryogel-like materials, which seem to be 2-fold or higher compared to other similar reports [33].

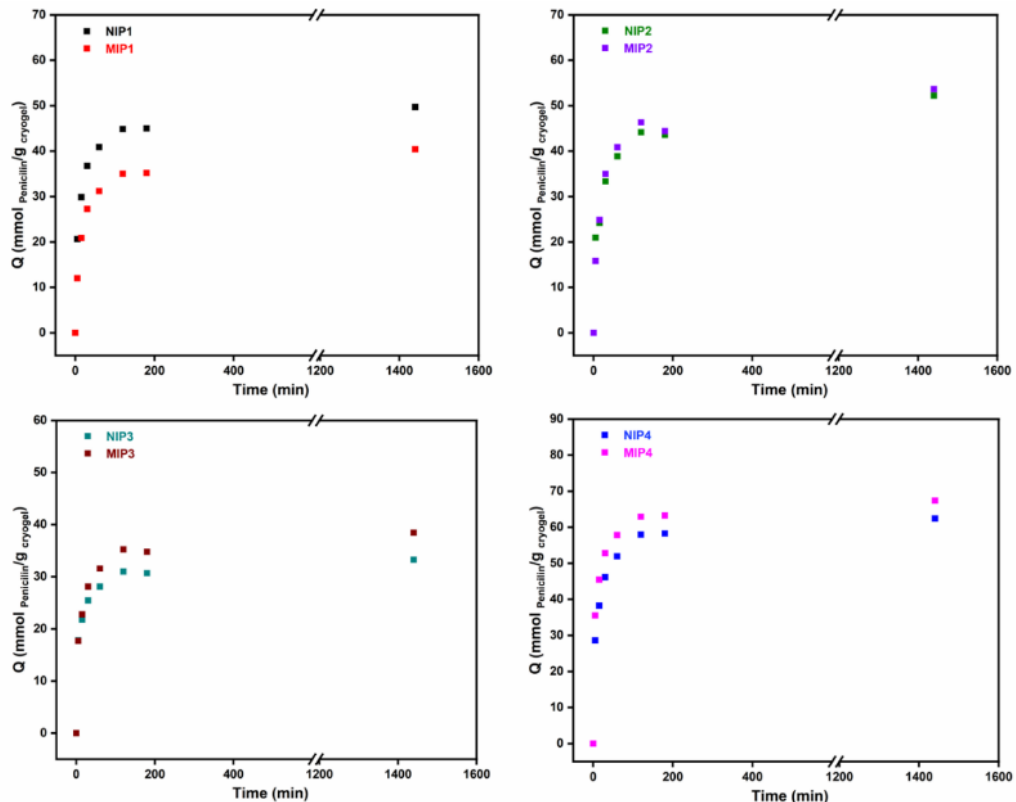


Fig. 3. The variance of adsorption capacities for MIP/NIP pairs in the time interval 0-1440 min

Furthermore, it seems that cryogel-like materials based on chitosan prepared in the laboratory were able to adsorb more specifically the PG vs. the reference NIPs. In this respect, the most significant IF values were recorded for samples MIP3 and MIP4, as highlighted in *Table 2*.

Thereby, the evaluation of IF in time shows that MIP1 has no specific adsorption vs. NIP1 (with all values of IF under 1), while MIP2 and MIP3 start to rebind PG specifically only after 15 min, with IF maxima registered at 60 min and 120 min, respectively. In the case of MIP4, the maximum IF was attained in the

first 5 min, after which the specificity slowly decreased at 1.079 when reaching 1440 min. Even though the IF values are moderate compared to recent studies on MIP gels [34], the results achieved in this study show that cryogel-like materials based on biocellulose and chitosan prepared in the lab are highly efficient for retaining high amounts of PG from water in the first 5 min of use. Which, in turn, may represent a “quick procedure” for PG retention.

**Table 2**  
**Specificity of rebinding evaluated by IF calculation**

Time (min)	IF			
	MIP1	MIP2	MIP3	MIP4
<b>5</b>	0.582	0.755	0.996	<b>1.240</b>
<b>15</b>	0.698	1.028	1.045	1.189
<b>30</b>	0.740	1.048	1.103	1.144
<b>60</b>	0.763	<b>1.051</b>	1.123	1.113
<b>120</b>	0.780	1.049	<b>1.137</b>	1.086
<b>180</b>	0.782	1.018	1.133	1.085
<b>1440</b>	0.813	1.026	1.125	1.079

Further on, the experimental values from Fig. 3 were analysed using a pseudo-second order kinetic model, in which case the adsorption capacity at 1440 min was used as equilibrium adsorption capacity. Eq. (4) [32] was used for the calculation of the kinetics adsorption parameters (summarized in Table 3) for samples based on commercial chitosan (NIP1, MIP1, NIP2, and MIP2 - model fitting in Fig. 4) and those based on chitosan prepared in the lab (NIP3, MIP3, NIP4 and MIP4- model fitting in Fig. 5).

**Table 3**  
**Characteristic parameters of the pseudo-second order kinetic model [32]**

Sample	$k_2$ (g mmol <sup>-1</sup> min <sup>-1</sup> )	$q_e$ (mmol/g)	$R^2$
NIP1	1.62*10-3	49.68	0.99993
MIP1	1.39*10-3	40.39	0.99989
NIP2	0.94*10-3	52.19	0.99968
MIP2	0.91*10-3	53.59	0.99970
NIP3	3.10*10-3	33.25	0.99995
MIP3	2.16*10-3	38.42	0.99992
NIP4	1.53*10-3	62.41	0.99997
MIP4	1.72 *10-3	67.34	0.99997

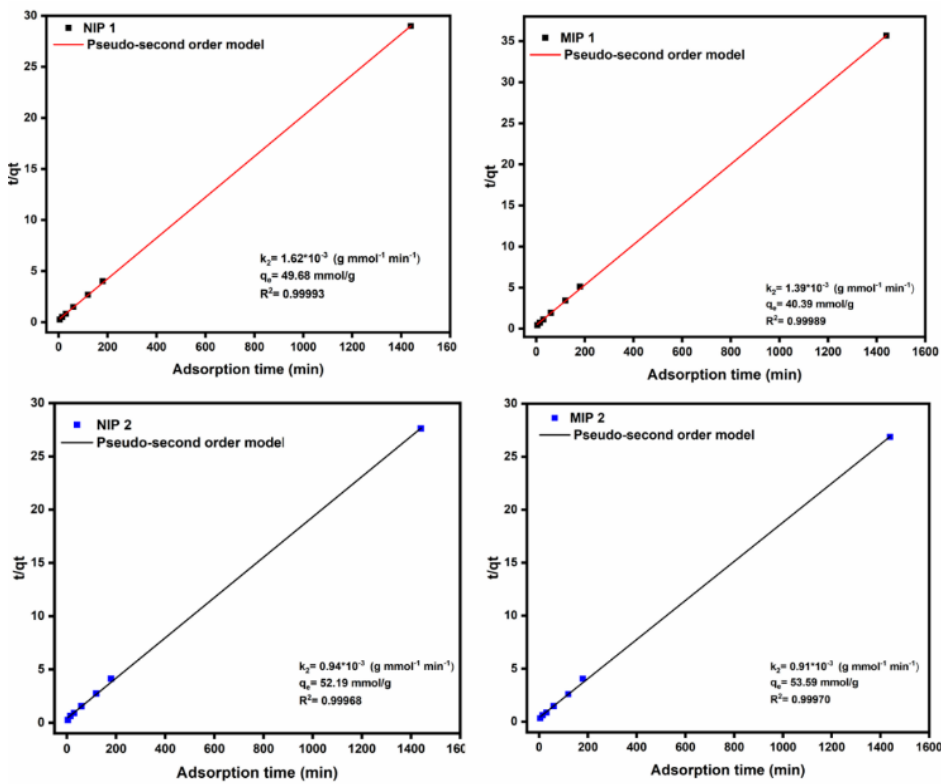


Fig. 4. Pseudo-second-order kinetics model of the adsorption process for NIP1/MIP1 and NIP2/MIP2 pairs

These results underline that the adsorption process of PG, by all the tested cryogel-like materials, follow a pseudo-second order kinetic with a linear relationship of  $t/q(t)$  vs.  $t$  and a high precision (all  $R^2$  values are above 0.999).

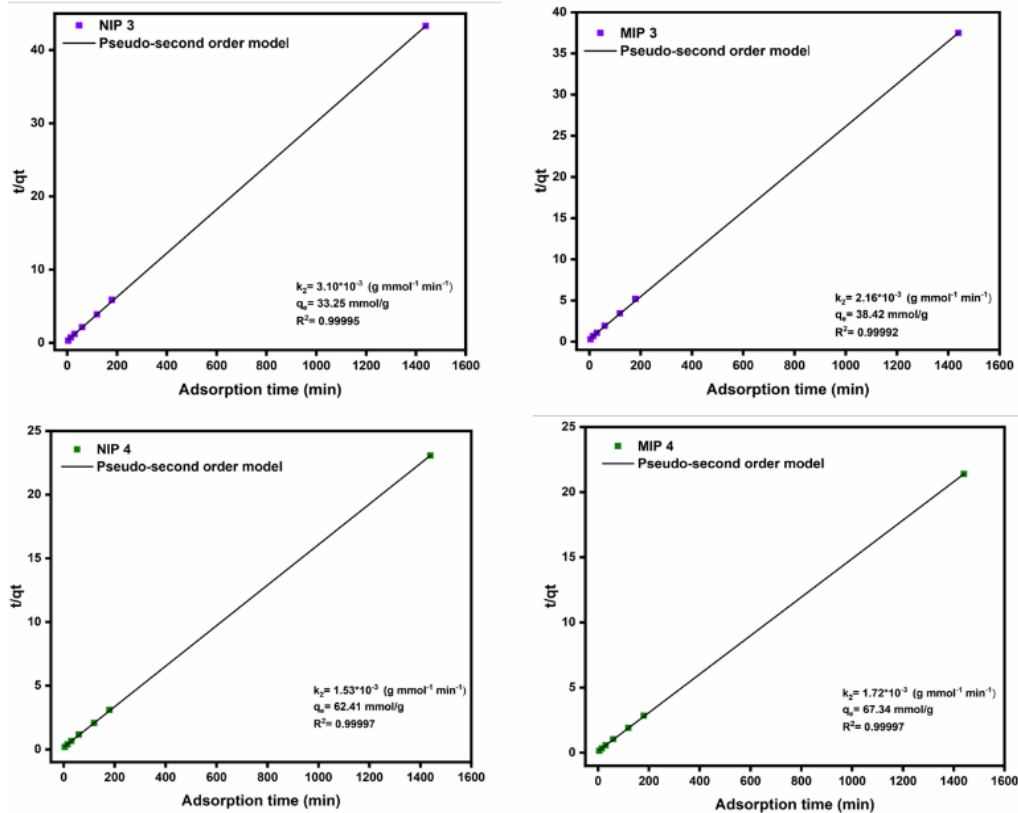


Fig. 5. Pseudo-second-order kinetics model of the adsorption for NIP3/MIP3 and NIP4/ MIP4 pairs

#### 4. Conclusions

This study was aimed at preparing molecularly imprinted cryogels-like materials for antibiotic retention, using natural polymers such as commercial chitosan or chitosan prepared in the lab from commercial chitin and biocellulose, as precursors. Meanwhile, PG antibiotic was used as a template molecule, with the end of developing specific binding sites for PG in the structure of the cryogel-like material, capable of recognizing and rebinding this analyte from aqueous solutions. In this respect, FTIR spectroscopy corroborated with the TGA/ DTG results have highlighted the presence of PG in the MIPs structure and, thus, confirming PG imprinting. The following swelling and rebinding studies revealed different behaviours of the MIP/NIP series of cryogel-like materials. For instance, the stability of cryogel-like materials in water was quite high accounting that the matrix was not chemically crosslinked, while the rebinding results have pointed out that all MIP cryogel-like materials are able to retain up to 2-fold more PG

compared to other studies. Yet, evaluating the specificity of adsorption, only three of the analysed MIPs retained PG in higher amounts compared to their reference NIP, the maximum value of  $IF = 1.24$  being recorded just after 5 min of contact with the PG solution, for the MIP cryogel based on biocellulose and chitosan prepared in the lab. The adsorption data of the process was fitted to a pseudo-second-order kinetic model, which proved to describe properly the investigated dependency.

### Funding

The authors would like to thank the EU and JPI Oceans, as well as the Romanian National Authority for Scientific Research and Innovation UEFISCDI (contract no.157/2020) for funding the project “Recycling crustaceans shell wastes for developing biodegradable wastewater cleaning composites BIOSHELL”, in the frame of the collaborative international consortium, financed under the ERA-NET Cofund BlueBio 2019. Marinela Dumitru also acknowledge the support of the Ministry of Investments and European Projects through the Human Capital Sectoral Operational Program 2014-2020, Contract no. 62461/03.06.2022, SMIS code 153735 (“OPTIM” project).

### R E F E R E N C E S

- [1]. *D. Cheng, et. al.*, A critical review on antibiotics and hormones in swine wastewater: Water pollution problems and control approaches, *Journal of Hazardous Materials*, **vol. 387**, 2020, 121682.
- [2]. *M. Javanbakht, et.al.*, Extraction and purification of penicillin G from fermentation broth by water-compatible molecularly imprinted polymers, *Materials Science and Engineering: C*, **vol. 32**, (8), 2012, pp. 2367-2373.
- [3]. *J. Cederfur, et. al.*, Synthesis and Screening of a Molecularly Imprinted Polymer Library Targeted for Penicillin G, *J. Comb. Chem.* **vol. 5**, 2003, pp. 67-72.
- [4]. *R. R. Pupin, et. al.* Magnetic molecularly imprinted polymers obtained by photopolymerization for selective recognition of penicillin G, *Journal of Applied Polymer Science*, **vol. 137**, 2019, 48496.
- [5]. *P. Weber, et.al.*, Nano-MIP based sensor for penicillin G: Sensitive layer and analytical validation, *Sensors and Actuators B* **vol. 267**, 2018, pp.26–33.
- [6]. *B. Sellergren, C. J. Allender*, Molecularly imprinted polymers: A bridge to advanced drug delivery, *Advanced Drug Delivery Reviews* **vol. 57**, 2005, pp. 1733–1741.
- [7]. *S. L. Ee, X. Duan, J. Liew, Q. Dzuy Nguyen*, Droplet size and stability of nano-emulsions produced by the temperature phase inversion method, *Chemical Engineering Journal* **vol. 140**, 2008, 626–631.
- [8]. *N. Barbani, et. al.*, Molecularly imprinted polymers by phase inversion technique for the selective recognition of saccharides of biomedical interest in aqueous solutions, *Polym Int* **vol. 66**, 2017, pp. 900–907.
- [9]. *E. Yeşilova, et.al.*, Molecularly imprinted particle embedded composite cryogel for selective tetracycline adsorption, *Separation and Purification Technology* **vol. 200**, 2018, pp. 155–163.

[10]. *M.V. Konovalova, et. al.*, Preparation and biocompatibility evaluation of pectin and chitosan cryogels for biomedical application, *Journal of Biomedical Materials Research*, **vol. 105**, 2017, pp. 547-556.

[11]. *A. Haleem, J.-M. Pan, A. Shah, H. Hussain, W.-D. He*, A systematic review on new advancement and assessment of emerging polymeric cryogels for environmental sustainability and energy production, *Separation and Purification Technology*, **vol. 316**, 2023, 123678.

[12]. *F. Ciuffarin, et.al.*, Interactions of cellulose cryogels and aerogels with water and oil: Structure-function relationships, *Food Hydrocolloids*, **vol. 140**, 2023, 108631.

[13]. *A.B. Karaduman, K. Çetin*, Molecularly Imprinted Cryogels for the Selective Adsorption of Salicylic Acid, *Applied Biochemistry and Biotechnology* **vol. 195**, 2023, pp.1877–1887.

[14]. *S. Zabihi, et.al.*, Preparation of molecular imprinted injectable polymeric micro cryogels for control release of mitomycin C, *Polymer Bulletin*, **vol. 80**, 2023, pp. 3883–3895.

[15]. *J. L. Urraca, et.al.*, A Stoichiometric Molecularly Imprinted Polymer for the Class-Selective Recognition of Antibiotics in Aqueous Media, *Angew. Chem.* **vol. 118**, 2006, pp. 5282 – 5285

[16]. *M. A. Söylemez, O. Güven*, Preparation and detailed structural characterization of Penicillin G imprinted polymers by PALS and XPS, *Radiation Physics and Chemistry*, **vol. 159**, 2019, 174-18.

[17]. *M. A. Soylemez*, Selective Removal of Penicillin G from Environmental Water Samples by Using Molecularly Imprinted Membranes, *Hittite Journal of Science and Engineering*, **vol. 7**, (4), 2020, pp. 329–337.

[18]. *E. Dellera, et. al*, Development of chitosan oleate ionic micelles loaded with silver sulfadiazine to be associated with platelet lysate for application in wound healing, *European Journal of Pharmaceutics and Biopharmaceutics* **vol. 88**, 2014, pp. 643–650.

[19]. *T. Piacham, C. I.-Na-Ayudhya, V. Prachayasittikul*, A simple method for creating molecularly imprinted polymer-coated bacterial cellulose nanofibers, *Chemical Papers* **vol. 68**, (6) 2014, pp. 838–841.

[20]. *C. Jantarat, et.al.*, Molecularly imprinted bacterial cellulose for sustained-release delivery of quercetin, *Journal of Biomaterials Science, Polymer Edition*, 2020.

[21]. *R. Jayakumar, D. Menon, K. Manzoor, S.V. Nair, H. Tamura*, Biomedical applications of chitin and chitosan-based nanomaterials—A short review, *Carbohydrate Polymers* **vol. 82**, 2010, 227–232.

[22]. *M. Burkatovskaya, et. al.*, Use of chitosan bandage to prevent fatal infections developing from highly contaminated wounds in mice, *Biomaterials* **vol. 27**, 2006, pp. 4157–4164.

[23]. *P. Dong, et.al.*, Macroporous zwitterionic composite cryogel based on chitosan oligosaccharide for antifungal application, *Materials Science & Engineering C* **vol. 128**, 2021, 112327.

[24]. *M.V. Dinu, et.al.*, Ice-templated hydrogels based on chitosan with tailored porous morphology, *Carbohydrate Polymers* **vol. 94**, 2013, pp.170– 178.

[25]. *M.V. Dinu, et.al.*, Synthesis, characterization and drug release properties of 3D chitosan/clinoptilolite biocomposite cryogels, *Carbohydrate Polymers* 2016, 153, 203–211.

[26]. *V.K. Mourya, N. N. Inamdar*, Chitosan-modifications and applications: Opportunities galore, *Reactive & Functional Polymers* **vol. 68**, 2008, pp. 1013–1051.

[27]. *H.S. Mansur, H. S. Costa*, Nanostructured poly(vinyl alcohol)/bioactive glass and poly (vinyl alcohol)/chitosan/bioactive glass hybrid scaffolds for biomedical applications, *Chemical Engineering Journal* **vol. 137**, 2008, 72–83.

[28]. *J.O. Mahony, et.al.*, Molecularly imprinted polymers—potential and challenges in analytical chemistry, *Analytica Chimica Acta* **vol. 534**, 2005, pp. 31–39.

- [29]. *A. Murei, et. al.*, Functionalization and antimicrobial evaluation of ampicillin, penicillin and vancomycin with Pyrenacanthagrandiflora Baill and silver nanoparticles, *Scientific Reports* 2020.
- [30]. *A. Miron, et. al.* Top-Down Procedure for Synthesizing Calcium Carbonate-Enriched Chitosan from Shrimp Shell Wastes. *Gels*, **vol. 8**, 2022, 742.
- [31]. *A. N. Frone, et. al.*, A. Bacterial cellulose sponges obtained with green cross-linkers for tissue engineering. *Mater. Sci. Eng. C* **vol. 110**, 2020, 110740.
- [32]. *D. Balarak, et.al.* Experimental and Kinetic Studies on Penicillin G Adsorption by Lemna minor, *British Journal of Pharmaceutical Research*, **vol. 9**, 2016, pp. 1-10.
- [33]. *M.V. Dumitru, et. al.*, Hybrid Cryogels with Superabsorbent Properties as Promising Materials for Penicillin G Retention. *Gels* **vol. 9**, 2023, 443. <https://doi.org/10.3390/gels9060443>.
- [34] *A. Zaharia, et. al.*, Molecularly Imprinted Ligand-Free Nanogels for Recognizing Bee Venom-Originated Phospholipase A2 Enzyme. *Polymers* **vol. 14**, 2022, 4200. <https://doi.org/10.3390/polym14194200>.
- [35]. *G.K. Kudaibergen, et.al.*, Study of the effect of temperature on the properties of gelatin-chitosan cryogels, *Bulletin of the University of Karaganda – Chemistry*, **vol. 2**, 2022, pp.4-11. <https://doi.org/10.31489/2022Ch2/2-22-4>.
- [36]. *Xu. Long, et.al.* Chitosan in Molecularly-Imprinted Polymers: Current and Future Prospects, *Int. J. Mol. Sci.* **vol. 16**, 2015, 18328-18347; <https://doi.org/10.3390/ijms160818328>.
- [37]. *Timothy M. A. Henderson, et.al.*, Cryogels for biomedical applications, *J. Mater. Chem. B*, **vol. 1**, 2013, pp. 2682.